

1 **An optimized reverse genetics system suitable for efficient recovery of simian, human**
2 **and murine-like rotaviruses**

3 Liliana Sánchez-Tacuba^{1,2,3}, Ningguo Feng^{1,2,3}, Nathan J. Meade^{4,5}, Kenneth H. Mellits⁵, Philippe
4 H. Jaïs⁶, Linda L. Yasukawa^{1,2,3}, Theresa K. Resch⁷, Baoming Jiang⁸, Susana López⁹, Siyuan
5 Ding^{10**} and Harry B. Greenberg^{1,2,3**}

6 ¹Department of Medicine, Division of Gastroenterology and Hepatology, Stanford School of
7 Medicine, Stanford, CA, USA; ²Department of Microbiology and Immunology, Stanford School of
8 Medicine, Stanford, CA, USA; ³VA Palo Alto Health Care System, Department of Veterans
9 Affairs, Palo Alto, CA, USA; ⁴Department of Microbiology-Immunology, Feinberg School of
10 Medicine, Northwestern University, Chicago, Illinois, USA; ⁵School of Biosciences, Division of
11 Microbiology, Brewing and Biotechnology, University of Nottingham, Sutton Bonington,
12 UK; ⁶Eukarÿs SAS, Pépinière Génopole, 4 rue Pierre Fontaine, 91000 Evry-Courcouronnes,
13 France; ⁷Cherokee Nation Assurance, Atlanta, GA, USA contracted to Division of Viral Disease,
14 Centers for Disease Control and Prevention, Atlanta, GA, USA, ⁸Division of Viral Diseases;
15 Centers for Disease Control and Prevention, Atlanta, GA, USA; ⁹Departamento de Genética del
16 Desarrollo y Fisiología Molecular, Instituto de Biotecnología, Universidad Nacional Autónoma de
17 México, Cuernavaca, México; ¹⁰Department of Molecular Microbiology, Washington University
18 School of Medicine, St. Louis, MO, USA.

19 **Co-corresponding authors: siyuan.ding@wustl.edu and hbgreen@stanford.edu

20

21 *The finding and conclusions in this report are those of the authors and do not necessarily*
22 *represent the official positions of Centers for Disease Control and Prevention.*

23

24 **ABSTRACT**

25 An entirely plasmid-based reverse genetics (RG) system was recently developed for
26 rotavirus (RV), opening new avenues for in-depth molecular dissection of RV biology,
27 immunology, and pathogenesis. Several improvements to further optimize the RG efficiency
28 have now been described. However, only a small number of individual RV strains have been
29 recovered to date. None of the current methods have supported the recovery of murine RV,
30 impeding the study of RV replication and pathogenesis in an in vivo suckling mouse model.
31 Here, we describe useful modifications to the RG system that significantly improve rescue
32 efficiency of multiple RV strains. In addition to the 11 RVA segment-specific (+)ssRNAs, a
33 chimeric plasmid was transfected, from which the capping enzyme NP868R of African swine
34 fever virus (ASFV) and the T7 RNA polymerase were expressed. Secondly, a genetically
35 modified MA104 cell line was used in which several compounds of the innate immune were
36 degraded. Using this RG system, we successfully recovered the simian RV RRV strain, the
37 human RV CDC-9 strain, a reassortant between murine RV D6/2 and simian RV SA11 strains,
38 and several reassortants and reporter RVs. All these recombinant RVs were rescued at a high
39 efficiency ($\geq 80\%$ success rate) and could not be reliably rescued using several recently
40 published RG strategies ($< 20\%$). This improved system represents an important tool and great
41 potential for the rescue of other hard-to-recover RV strains such as low replicating attenuated
42 vaccine candidates or low cell culture passage clinical isolates from humans or animals.

43 **IMPORTANCE**

44 Group A rotavirus (RV) remains as the single most important cause of severe acute
45 gastroenteritis among infants and young children worldwide. An entirely plasmid-based reverse
46 genetics (RG) system was recently developed opening new ways for in-depth molecular study
47 of RV. Despite several improvements to further optimize the RG efficiency, it has been reported

48 that current strategies do not enable the rescue of all cultivatable RV strains. Here, we
49 described helpful modification to the current strategies and established a tractable RG system
50 for the rescue of the simian RRV strain, the human CDC-9 strain and a murine-like RV strain,
51 which is suitable for both *in vitro* and *in vivo* studies. This improved RV reverse genetics system
52 will facilitate study of RV biology in both *in vitro* and *in vivo* systems that will facilitate the
53 improved design of RV vaccines, better antiviral therapies and expression vectors.

54

55

56 INTRODUCTION

57 Despite the introduction of multiple safe and effective rotavirus (RV) vaccines such as the
58 widely licensed Rotarix and RotaTeq vaccines, species A RVs remain the single most important
59 cause of severe acute gastroenteritis among infants and young children worldwide (1). RVs
60 are responsible for between 128,000 and 215,000 deaths each year, primarily in developing
61 countries (2). RVs belong to the *Reoviridae* family, comprising a variety of icosahedral,
62 nonenveloped multi-segmented double-stranded (ds) RNA viruses. RVs have three concentric
63 layers of protein that surround an RNA genome, which contains 11 dsRNA segments encoding
64 six structural (VP1-VP4, VP6, VP7) and six nonstructural (NSP1-NSP6) proteins (3).

65 While our understanding of RV epidemiology, clinical course, pathophysiology, immunology
66 and replication strategy has increased substantially over the last 40+ years, important questions
67 about complex and multifaceted processes such as host-range restriction, determinants of
68 virulence and immune correlates of protection are still poorly understood (3-6). However, due to
69 the recent introduction of an efficient reverse genetics (RG) system for RVs (7), we now have a

70 powerful investigative tool to effectively explore these and other long standing questions
71 regarding RV biology. Kanai and collaborators first established an entirely plasmid-based RG
72 system for the simian RV SA11 strain (7). This virus was originally isolated in 1958 (8), is very
73 well adapted to cell culture, and has been used as a prototype strain in many RV studies over
74 the ensuing years (9). While it is capable of infecting a variety of animals including primates (10)
75 and mice (11), it is not highly pathogenic and does not spread efficiently from host-to-host in
76 experimental animal systems. In the Kanai RG system, 11 plasmids encoding each of the SA11
77 gene segments are co-transfected with helper plasmids encoding the reovirus fusion-associated
78 small transmembrane (p10 FAST) protein and the vaccinia virus capping enzymes into BHK-T7-
79 expressing cells. Following an MA104 cell overlay and inoculation of the mixed cell lysates from
80 the transfected BHK-T7 cells onto fresh MA104 cells, infectious RVs are recovered (7). After
81 this report, there have been several additional descriptions of the RG system adapted for the
82 rescue of two human RV strains: KU (12) and Odelia (13). The rescue of several recombinant
83 viruses based on an SA11 genetic backbone, some carrying heterologous RV gene segments
84 encoding VP4 and VP7 (14, 15), others carrying engineered segments 5 or 7 with associated
85 reporter genes have also been reported (7, 16-18). All these reports described some
86 modifications of the original rescue protocol that purported to further improve the efficiency
87 and/or utility of the original RG system.

88 The suckling mouse is currently the best-established and widely used small animal model
89 system for studying RV infection *in vivo* (4, 19, 20). This model faithfully recapitulates several
90 aspects of RV infection in human infants: suckling mice are highly susceptible to murine RV
91 infection and develop severe diarrhea following low titer inoculating doses of homologous
92 murine RVs, while immuno-competent adult mice, like adult humans are more resistant to RV
93 induced diarrheal disease. Of note, heterologous RVs (non-murine RV such as the SA11 strain)

94 can infect suckling and adult mice but replicate poorly, do not cause diarrhea when
95 administered at low titers, and do not spread efficiently from host to host. In infant mice, cultured
96 intestinal epithelial cells, and human organoid culture systems an important part of the host
97 ability to restrict RV replication efficiently is mediated by innate immune response (21-23).
98 Furthermore, characterization of the replication of murine and non-murine RV strains in the
99 suckling murine host and in cultured cells has allowed the identification of several highly
100 effective mechanisms that homologous viruses use to evade the host innate antiviral response
101 (4, 20, 24-26).

102 Murine RVs have proven difficult to adapt to cell culture without losing virulence. In addition,
103 in general, when adapted they replicate poorly in cell culture, in the range of $1-5 \times 10^5$ plaque
104 forming units (PFUs)/mL (27, 28) making them difficult to rescue using the current RG
105 strategies. Many human RV isolates also replicate less robustly than a variety of animal strains
106 and even some animal RV strains have been difficult to rescue despite their robust replication
107 ability. For these reasons, we sought to develop a modified, more reproducible and efficient RG
108 protocol for RV, which relies on the inclusion of a recently described "Chimeric Cytoplasmic
109 Capping-Prone Phage Polymerase" (C3P3-G1) (29) as well as a genetically modified MA104
110 cell line. This new protocol enables a more efficient recovery of some human, simian and
111 murine-like RV strains that had previously proven difficult to rescue using current RG
112 strategies.

113 RESULTS

114 Generation and characterization of an IRF3 and STAT1 defective MA104 cell line.

115 Interferons (IFNs) are key components of the innate host defense against many viruses
116 including RV (4, 24, 30-32). Although MA104 cells are believed to have a blunted IFN response
117 and this feature plus other characteristics has made them a highly permissive cell substrate for

118 RV propagation (33), we reasoned that disarming IFN signaling in MA104 cells might enhance
119 RV replication and RG recovery rates. We took advantage of the parainfluenza virus 5 (PIV5,
120 previously SiV5) V protein and the bovine viral diarrhea virus (BVDV) N protease, which target
121 the signal transducer and activator of transcription 1 (STAT1) (34, 35) and the interferon
122 regulatory factor 3, also known as IRF3 (36, 37) respectively for degradation. In addition to the V
123 protein's ability to prevent the antiviral response by degrading STAT1, its ability to disarm the
124 RNA sensing pathway by disrupting the RIG-I and MDA-5 activation has been reported (38, 39).
125 Of note, RIG-I and MDA-5 are known to mount an early interferon response to RV infection (40).
126 We expressed PIV5 V and BVDV N proteins, either individually or in combination in MA104
127 cells, as previously described (41). Protein levels of STAT1 and IRF3 were examined by
128 western blot to confirm functionality-expression of N and V proteins in MA104 stable cell lines
129 (dual-expressing cells designated as MA104 N*V cells) (Fig 1A).

130 We next treated the MA104 N*V cells with IFN- α to assess their ability to respond to exogenous
131 type I IFNs (IFN-I) (Fig 1B). Wild-type (wt) MA104 cells responded to IFN- α treatment, with rapid
132 phosphorylation of STAT1 (tyrosine 701), followed by induction of canonical interferon-
133 stimulated genes (ISGs) including the Myxovirus resistance protein 1 (MX1) and the interferon-
134 induced transmembrane protein 3 (IFITM3) proteins (Fig 1B). In contrast, there was a complete
135 loss of STAT1 phosphorylation in MA104 N*V cells (Fig 1B). In addition, neither IFITM3 nor
136 MX1 levels increased following IFN- α treatment (Fig 1B). Collectively, these data indicated that
137 the MA104 N*V cells have a diminished response to IFN- α .

138 **Inhibition of IRF3 and STAT1 responses in MA104 cells enhances the replication of**
139 **several RV strains.**

140 We next examined the ability of several human and animal RV strains to replicate in the
141 wtMA104 as compared to MA104 N, V, or N*V cells. All 5 RV strains tested replicated to
142 significantly higher virus titers in the MA104 N*V cells (Fig 2A). While some RV strains (e.g.

143 RRV and SA11) showed only modest, but significant ($p \leq 0.05$) increases, the human CDC-9
144 strain, a new RV vaccine candidate strain (42), had an almost 10-fold enhancement in viral yield
145 in the MA104 N*V cells (Fig 2A). For two murine RV strains (ETD and D6/2), we also observed
146 significant increases in viral titers (~5-fold). Taken together, these findings demonstrate that the
147 MA104 N*V cells have lower levels of endogenous IRF3 and STAT1 and these lower levels are
148 associated with significantly enhanced replication capacity of selected human, simian and
149 murine RV strains.

150 In addition to virus titers, we compared RV mRNA levels in wtMA104 and MA104 N*V
151 infected cells, with or without IFN- α pretreatment (Fig 2B). No difference was observed in RV
152 NSP5 mRNA levels in MA104 N*V cells in the presence or absence of IFN- α . In contrast, the
153 replication of an IFN sensitive RV strain (such as UK bovine RV (40) was decreased by 1 Log₁₀
154 post IFN- α stimulation of wtMA104 cells (Fig 2B). Interestingly, we found that, for the human
155 CDC-9 strain, pre-treatment of wtMA104 cells with IFN- α (Fig 2B) did not suppress RV
156 replication. Nevertheless, the level of CDC-9 mRNA was higher (~10X) in the STAT1/IRF3
157 modified MA104 N*V cells as compared to wtMA104 (Fig 2B). Based on these findings, we
158 hypothesized that the modified MA104 N*V cells may be a better cell substrate than wtMA104
159 cells to enhance the RG recovery of some RV strains.

160 **The MA104 N*V cell line enhances the RG recovery of the human rCDC-9 RV.**

161 Since the MA104 N*V cell line supported higher levels of replication for several RV strains,
162 we next assessed their ability to enhance RG rescue efficiency. Using the RG system described
163 by Komoto (12) as a reference, MA104 N*V cells enabled an efficient rescue of the human
164 CDC-9 strain (10 rescues in 10 attempts). In contrast, when wtMA104 cells were used instead,
165 only 3 of 10 attempts resulted in the recovery of replication competent rCDC-9 virus.
166 Additionally, the hard-to-rescue simian RRV strain was not rescued using wtMA104 cells (0 out
167 of 6 attempts), but when MA104 N*V cells were used, rRRV could be rescued at low efficiency

168 (1 out of 3 attempts). These findings indicate that at least for some RV strains, the use of
169 modified MA104 N*V cells improves the efficiency of the RV RG system.

170 **RNA capping enzyme and T7 polymerase fusion protein further increases RV RG**
171 **efficiency.**

172 With MA104 N*V cells, we were able to rescue rRRV but at a low efficiency. In an attempt to
173 further improve the RG system, we next added to the system an engineered chimeric protein
174 (C3P3-G1) consisting of the African swine fever virus NP868R capping enzyme and the T7
175 DNA-dependent RNA polymerase (29). An earlier version of this plasmid had previously been
176 shown to enhance the reovirus RG system success rate by approximately 100-fold (43). Such
177 an increase in viral titer was explained by the capping of mRNA produced with this system,
178 which enhances protein expression as well as assembly and RNA incorporation into reovirus
179 virions (43). The inclusion of a cytomegalovirus support plasmid for the African swine fever virus
180 NP868R capping enzyme in a modified RVA RG system has been reported (16). With this
181 NP868R-based system, some recombinant rotavirus with a genetically modified segment 7
182 dsRNA were successfully rescued (16, 18). Nevertheless, the rescue efficiency of murine-like
183 RV, such rD6/2 like (1) (see below) did not show an improvement using this NP868R-based
184 system.

185 We next tested the rescue of the simian RRV strain using the modified Komoto RG system with
186 or without C3P3-G1 supplementation at a 2:1 ratio along with the other 11 RRV plasmids.
187 Inclusion of C3P3-G1 substantially increased the efficiency of rRRV rescue from 0/6 to 3/3.
188 Hence, simply including the C3P3-G1 plasmid to the RV RG protocol significantly ($p \leq 0.05$)
189 increased the efficiency of rRRV recovery in wtMA104 cells.

190 **An RG system for the recovery of recombinant murine-like RVs.**

191 So far, we have shown that either MA104 N*V cells or C3P3-G1 plasmid alone can
192 significantly enhance RG rescue of a human or a simian RV strain. To test for potential synergy,

193 we attempted the RG rescue of a previously well-characterized, cultivatable and murine virulent
194 reassortment RV (designated D6/2) derived from a mouse pup co-infected with the non-cell
195 culture adapted EW strain of murine RV and the RRV strain of simian RV (20, 24). This
196 reassortant contains 10 of 11 murine EW strain genes and the 4th gene encoding VP4 from
197 RRV. The D6/2 strain induces diarrhea in suckling pups, transmits between littermates, and
198 replicates moderately well in cell culture (24). However, despite numerous attempts (>10), D6/2
199 could not be successfully rescued. We postulated, based on previous genetic analysis (24)
200 and monoessortants between SA11 and D6/2 (Supplementary Figure 1), that substituting
201 SA11 genes 1 and 10 into a molecular D6/2-based recombinant murine RV might possess a
202 similar virulence phenotype as the naturally occurring murine D6/2 reassortant but be more
203 amenable to RG rescue.

204 Rescue of a rD6/2 like (1) RV; genes 2,3,5,6,7,8,9,11 from the parental wt non-cultivable
205 murine EW parental strain, gene 4 from RRV and genes 1 and 10 from SA11, was carried out
206 as described by the Komoto RG system with modifications, or by including the C3P3-G1, or by
207 replacing wtMA104 cells with the MA104 N*V cells, or by using both modifications together. We
208 found that, although the addition of the C3P3-G1 plasmid alone, or the substitution of the
209 MA104 N*V cells alone, boosted recovery efficiencies, rescue was most efficient, when both,
210 the C3P3-G1 plasmid and the modified cell line were used together (Table 1). Based on these
211 results, we propose a new system for the rescue of murine-like RV and other hard-to-rescue RV
212 strains, as described in detail in the Material and Methods section and is summarized in Figure
213 3.

214 **Multiple reporter rRVs were rescued using the optimized RG system.**

215 To provide additional proof-of-concept that this optimized RV RG protocol provides major
216 advantages over other current systems (in modified versions), we directly compared the rescue
217 efficiency of this enhanced system to those described by either Komoto *et al.* or by Kanai *et al.*

218 ([7](#), [12](#)) with modifications. For this purpose, we tested the rescue efficiency of all recombinant
219 RVs described above, including the simian RRV strain, the human CDC-9 strain, and the rD6/2
220 like (1) RV. We also included a few more genetically modified rRVs, such as a GFP expressing
221 RRV (GFP and NSP3 separated by a P2A element on gene segment 7. Fig 5A) and a mono-
222 reassortment of VP4 derived from the bovine RV UK strain on the human CDC-9 backbone
223 (rCDC-9/UK_VP4). These particular RVs had not been consistently “rescuable” by us or others
224 (personal communications) using standard RG strategies and served as additional examples
225 to test whether the improved system allowed the efficient rescue of recombinant RVs bearing
226 heterologous gene segments or engineered reporter genes.

227 The modified Kanai and the Komoto protocols rescue recombinant SA11 very efficiently (Table
228 1). However, rescue frequency of the recombinant human CDC-9 strain was very low using
229 either the Kanai or Komoto modified protocols (0/2 and 0/8 respectively) and a recombinant
230 RRV strain was either not isolated (0/2) or isolated only rarely (1/6) using the modified Kanai or
231 Komoto protocols respectively. Similarly, neither of these modified RG protocols were
232 particularly efficient for the rD6/2 like (1) RV, when compared to the improved protocol, which
233 included both the MA104 N*V cells and the C3P3-G1 plasmid (Table 1). In all comparisons,
234 these rescue improvements were significantly more efficient than the other modified protocols
235 ($P < 0.01$).

236 To validate the genomic RNA migration patterns of the rescued recombinant RVs, the
237 dsRNA genomes were isolated and examined by RNA polyacrylamide gel electrophoresis
238 (PAGE). The dsRNA genome profiles for all recovered recombinant RVs using the optimized
239 RG system are shown in Fig 4. The dsRNA migration patterns between wt and recombinant
240 viruses were identical for all the RV strains recovered. For the rD6/2 like (1) RV, the genome
241 profiles confirmed that segments 1 and 10 originated from SA11 and the remaining nine from
242 the D6/2 RV. The mono-reassortment containing bovine RV UK strain VP4 on the CDC-9
243 backbone showed the same migration dsRNA pattern as wtCDC-9, except for segment 4, which

244 co-migrated with UK segment 4. Finally, RNA-PAGE was used to identify the modified segment
245 7 from rRRV-GFP (Fig 4 and 5C), which was additionally confirmed by sequence analysis (data
246 not shown). Altogether, these findings corroborate the identities of all the recombinant RVs
247 rescued and document the enhanced efficiency of the improved RG protocol for a wide variety
248 of RV strains that had proven difficult to rescue using conventional protocols.

249 The genetic stability of the rescued recombinant RVs was assessed (Fig 5B and 5C) by 5X
250 serial passage (p1-p5) in wtMA104 cells and the recombinant progenies from each passage
251 were titrated by a standard focus forming assay. Virus titers generally increased in the first two
252 passages (Fig 5B), and then remained stable. The multi-step growth kinetics (Fig 5D) of
253 recombinant RVs and their plaque sizes (Fig 5E) in wtMA104 cells were also examined and
254 were not statistically different from their parental strains. Interestingly, the rD6/2 like (1) RV,
255 which, unlike the D6/2 prototype, harbored 2 genes from SA11, did not show statistically
256 significant differences in its *in vitro* growth characteristics compared to the D6/2 parental strain.
257 But the rRRV-GFP virus that carries an engineered segment 7, although it showed a similar
258 growth curve to the wtRRV, formed smaller plaques than its parental strain (Fig 5E). The same
259 phenotype was also observed for other recombinant RVs carrying fluorescent reporters such as
260 rSA11-GFP, rSA11-mCherry (17) and rSA11-UnaG (16). GFP signals were exclusively
261 observed in rRRV-GFP infected RV antigen VP6 positive cells (Fig 5F). This rRRV-GFP virus
262 was stable over 8 passages in wtMA104 cells (Fig 5C).

263

264 **Recombinant RVs replicate in the intestine and cause diarrhea *in vivo***

265 Finally, to determine whether rRRV and rD6/2 like (1) RV are able to infect mice as their wtRV
266 counterparts do, the replication, spread, and pathogenesis of these recombinant RV were
267 studied in an *in vivo* mouse model (44). Litters of 4 to 5-day-old mice were orally inoculated with
268 doses of 1×10^4 PFUs of rD6/2 like (1) or D6/2, or 1×10^7 PFUs of rRRV or wtRRV. Assessment

269 of diarrhea by standard diarrhea scores and intestinal replication as measured by fecal RV
270 shedding by RT-qPCR (45) were monitored. We observed virtually identical fecal shedding and
271 diarrhea curves of wtRRV and rRRV following infection (Fig 6A, 6B).

272 As is shown in Fig 6C and 6D, shedding curves between rD6/2 like (1) vs D6/2 did not show
273 significant difference. Further, we found that the rD6/2 like (1) RV induce diarrhea and can
274 spread just as the D6/2 does, since we observed that the non-infected pups (mock) kept in the
275 same cage as RV infected pups developed diarrhea on 3 to 4 dpi (Fig 6D) and their feces,
276 collected at day 5-8 pi, was positive for mRNA NSP5 as detected by RT-qPCR. In order to
277 further characterize the infection in the mouse pups, the dsRNA migration pattern of rD6/2-like
278 (1) RV was analyzed. RV was isolated from stools collected between day 2-4 of rD6/2-like (1)
279 RV mice-infected and after 3 serial passages on MA104 cells, a portion of the extracted dsRNA
280 from the cells was electrophorized (Fig 6E). Taken together, these results support the
281 conclusion that recombinant RVs exhibit the same *in vivo* phenotype as their corresponding
282 wtRV counterparts. As anticipated and consistent with previous characterizations (20, 24, 25)
283 rD6/2-like (1) was able to efficiently infect mice, induce diarrhea, and spread to uninfected litter
284 mates in a manner similar or identical to D6/2 RV.

285 **DISCUSSION**

286 In this study, we made several significant modifications of the current RV RG system and
287 evaluated whether these modifications improved rescue efficiency for certain RV strains. By
288 adding the recently described C3P3-G1 plasmid (29) along with using genetically modified
289 MA104 N*V cells with reduced capacity to mount an antiviral IFN response, we developed a
290 more efficient and consistently successful ($\geq 80\%$) RV RG protocol that allowed the recovery of
291 several recombinant RVs that current RG strategies did not efficiently permit. The precise
292 mechanisms by which the use of C3P3-G1 and of the modified MA104 N*V cell line allowed
293 enhanced rescue efficiency are not known. Although the full relevance of the CAP structure to

294 the RV replication cycle is not well understood, the enhanced capping activity provided for the
295 C3P3-G1 system seems to be useful. On the other hand, although BHK-T7 constitutively
296 expresses T7 polymerase, an increased amount of this polymerase provided by transient C3P3-
297 G1 transfection, could also be responsible for higher levels of pT7-RV plasmid transcription. The
298 disrupted IFN-I response at several levels in the modified MA104 N*V seems likely to be
299 involved in the capacity of this line to facilitate the RV rescue. If so, this benefit could be strain
300 specific, since the ability of different RV strains to effectively counter the IFN response at
301 different levels is documented ([4](#), [31](#)).

302 Our findings indicate that the rescued RVs are genetically stable and showed similar replication
303 phenotypes to their corresponding wtRV parents. In addition, we determined that an RRV
304 carrying a GFP reporter and a human CDC-9 harboring a heterologous UK VP4 segment can
305 be efficiently rescued and remain genetically stable.

306 We established a tractable RG system for the rescue of the simian RRV strain, a prototype
307 simian RV used as an experimental model for numerous *in vivo* and *in vitro* studies
308 ([4](#), [19](#), [20](#), [24](#)). With this improved system, the reliable rescue of recombinant RVs based on an
309 RRV genetic background is now feasible. In addition, data from suckling mice infection with
310 wtRRV vs rRRV, demonstrate that rRRV is capable of infecting mice and producing diarrhea in
311 a manner similar to wtRRV. These rRRV or RRV genetic background viruses, can now be used
312 in future studies to better understand the genetic basis of systemic RV spread ([24](#), [46](#)), RV
313 associated biliary disease ([47-49](#)), and heterotypic immunity ([50](#)).

314 We also described the rescue via RG of the CDC-9 human RV strain, currently being evaluated
315 as a potential inactivated human RV vaccine candidate. This strain was first isolated from fecal
316 specimens and then adapted to grow in Vero cells and it has been shown to be safe,
317 immunogenic, and effective at inducing immunity against severe RV disease in several animal
318 models ([42](#), [51](#)). The role of the individual RV proteins as contributors to the protective efficacy

319 of CDC-9 can now be directly examined in relevant animal models using selected
320 monoreassortants (Supplementary Figure 1). Notwithstanding some initial difficulties, we were
321 able to rescue a recombinant murine-like RV (reassortment RV: genes 2,3,5,6,7,8,9,11 from the
322 parental wt murine EW strain, gene 4 from RRV and genes 1 and 10 from SA11) which is called
323 rD6/2 like (1). Prior publications from our lab demonstrated that the host-range restricted murine
324 RV replication phenotype in the mouse intestine is primarily attributed to gene segments 4 and 5
325 and does not involve genes 1 and 10 (24). As we expected this *bona fide* murine RV was
326 able to efficiently infect mice, produce diarrhea and spread to uninfected litter mates similar to
327 as a murine RV.

328 The new RG capability will now permit us to study the mechanisms and viral determinants of
329 host range restriction, tissue tropism and systemic spread in mice in much greater detail and
330 depth and we plan to actively pursue these areas in future studies.

331 MATERIALS AND METHODS

332 **Cell culture and viruses:** The *Cercopithecus aethiops* epithelial cell line MA104 (ATCC CRL-
333 2378) was grown in Medium 199 (Sigma-Aldrich) supplemented with 10% heat-inactivated fetal
334 bovine serum (FBS), 100 I.U. penicillin/mL, 100 µg/mL streptomycin and 0.292 mg/mL L-
335 glutamine (complete medium). A Baby Hamster Kidney fibroblast cell line stably expressing T7
336 RNA polymerase BHK-T7, was kindly provided by Dr. Ursula Buchholz (Laboratory of Infectious
337 Diseases, NIAID, NIH, USA) and previously described (52). This cell line was cultured in
338 complete (10% FBS, 100 I.U. penicillin/mL, 100 µg/mL streptomycin and 0.292 mg/mL of L-
339 glutamine) Dulbecco's modified Eagle's medium (DMEM) and 0.2 µg/mL of G-418 (Promega)
340 was added to the complete medium at every other passage. MA104*N, MA104*V and MA104
341 N*V stable cell lines were generated from MA104 cells as described previously (41) and
342 cultured in complete medium 199 in the presence of puromycin (5 µg/mL), blasticidin (5 µg/mL)

343 and puromycin (3 µg/mL) + blasticidin (3 µg/mL) respectively. Both antibiotics were purchased
344 from InvivoGen, San Diego, CA. Cells were stimulated with human IFN-α A/D (800 UI/mL) for 30
345 min or 16 h for either western blot or RV replication studies, respectively.

346 The wtRV strains used in this study include simian RRV (G3P[3]) ([53](#)), and SA11(G3P[2]) ([53](#)),
347 human CDC-9 P50 (G1P[8]) ([42](#)), bovine UK (G6P[5]) ([53](#)), and the murine reassortant D6/2.
348 These and other recombinant RVs were propagated in wtMA104 cells as described ([54](#)). Prior
349 to infection, all RV inocula were activated with 5 µg/mL of trypsin (Gibco Life Technologies,
350 Carlsbad, CA) for 30 min at 37°C.

351 **Plasmids.** The simian SA11 plasmid collection: pT7-VP1SA11, pT7-VP2SA11, pT7-VP3SA11,
352 pT7-VP4SA11, pT7-VP6SA11, pT7-VP7SA11, pT7-NSP1SA11, pT7-NSP2SA11, pT7-
353 NSP3SA11, pT7-NSP4SA11, and pT7-NSP5SA11 as well the three helper plasmids pCAG-
354 D1R, pCAG-D12L and pCAG-FAST-p10 were originally made by Dr. Takeshi Kobayashi
355 (Research Institute for Microbial Diseases, Osaka University, Japan) and obtained from
356 Addgene ([7](#)). The whole murine pT7-D6/2 plasmid collection and the pT7-UKVP4 were
357 commercially synthesized (GenScript USA Inc.) The complete simian pT7-RRV plasmid
358 collection was originally constructed by Dr. Susana Lopez (UNAM, Mexico City, Mexico). The
359 modified pT7-RRV-NSP3 (see Fig 5A) was engineered following a validated approach
360 previously described ([16](#), [18](#)). The plasmid constructs for individual genes of RV CDC-9 strain at
361 passage 11 in MA104 cells were provided by Dr. Baoming Jiang (CDC, Atlanta, USA) ([55](#)). The
362 purification of all the plasmids was performed using QIAGEN Plasmid Miniprep kit per
363 manufacturer's instructions. To validate all the new pT7-RV plasmids, a panel of SA11 × CDC-9
364 or RRV or D6/2 monoreassortant viruses on the strain SA11 genetic background were
365 generated following the Komoto *et al* ([12](#)) procedure with the following modifications or the
366 improved RG protocol (see below and Supplementary Figure 1).

367 **Generation of recombinant rotaviruses:** Recombinant RVs were generated as described by
368 Kanai *et al.* (7) or Komoto *et al.* (12) with some modifications. For Kanai protocol 7.5-8.5 x
369 10⁴ BHK-T7 cells were seeded in 12-well plates, 48 h after cells were cotransfected with 0.4 µg
370 of either RV rescue plasmid (1-fold), 0.0075 µg of pCAG-FAST, and 0.4 µg of each capping
371 enzyme expression plasmid using 2 µL of TransITLT1 (Mirus) transfection reagent per
372 microgram of plasmid DNA. After plasmid transfection, all the transfected cells were processed
373 as described below. The original Komoto protocol was modified as indicated: confluent
374 monolayers of BHK-T7 cells, seeded in 12-well plates (see conditions above) were transfected
375 with 0.4 µg of either RV rescue plasmid (1-fold), with 3-fold increased amounts of the two
376 plasmids carrying the NSP2 and NSP5 genes (1.2 µg/well) using 3 µL of TransIT-LTI
377 transfection reagent per µg of plasmid DNA, the transfected BHK-T7 cells were then processed
378 as described below.

379 The improved protocol is described in brief: using 1-well of a 12-well plate as a reference, 7.5
380 X10⁴ BHK-T7 cells were resuspended in 1 mL of complete DMEM (10% heat inactivated SFB,
381 100 I.U./mL penicillin, 100 µg/mL streptomycin, 0.292 mg/mL) G418-free medium and seeded
382 into the well. Forty-eight hours later, the medium was replaced by 800 µL of fresh complete
383 DMEM medium, and then the sub-confluent BHK-T7 monolayer was transfected with the
384 corresponding transfection mix that contained 125 µL of prewarmed Opti-MEM, 400 ng each of
385 the 11 RVA pT7 plasmid, except pT7-NSP2 and pT7-NSP5 which were added at 1200 ng, and
386 800 ng of the plasmid pCMVScript-NP868R-(G4S)4-T7RNAP (C3P3-G1). As transfection
387 reagents, 14 µL of Trans IT-LTI (Mirus Bio LLC) were used. All the plasmids and transfection
388 reagents were mixed in a pipet by gently moving it up and down and then incubated at room
389 temperature for 20 min. After this time, the transfection mixture was added drop by drop to the
390 medium of BHK-T7 monolayers and then the cells were returned to 37°C. 16-18 hours later,
391 two washes with FBS-free medium were done after which 800 µL of serum-free DMEM was

392 added to the transfected-BHK-T7 cells. Twenty-four hours later, 5×10^4 wtMA104 (modified
393 Kanai and Komoto protocols) or MA104 N*V cells (improved protocol) in 200 μ L of serum-free
394 DMEM was added to the well, along with 0.5 μ L/mL of porcine pancreatic type IX-S trypsin
395 (Sigma-Aldrich). MA104 N*V and BHK-T7 cells were co-cultured for 72 hours, after which they
396 were frozen and thawed three times. To remove cell debris, the lysate was centrifuged at 350 x
397 g for 10 min at 4°C and then activated with 2.5 μ g/mL of trypsin to infect a 3-day old monolayer
398 of MA104 cells. After 1h of adsorption, the inocula were removed and 1 mL of serum-free
399 medium supplemented with 0.5 μ g/mL of trypsin was placed on the cells. MA104 cells were
400 incubated at 37°C for 5 days or until cytopathic effects were observed (passage 1). We defined
401 as successfully rescue virus, when MA104 cells infected with the corresponding RV rescued
402 passage 1 were positive by immunostaining using an anti-DLPs antibody (see section of focus-
403 forming assay).

404 **Plaque and focus-forming assays:** Culture supernatant or virus samples were serially diluted
405 2 or 10-fold and added to a monolayer of MA104 cells for 1 h at 37 °C. Samples were removed
406 and replaced with 0.1% agarose (SeaKem® ME Agarose. Lonza) in M199 serum free medium
407 supplement with 0.5 μ g/ mL of trypsin. Cultures for plaque assay were incubated for 2-5 days at
408 37 °C, then fixed with 10% formaldehyde and stained with 1% crystal violet (Sigma-Aldrich) to
409 visualize plaques. Cultures for focus forming assay were incubated for 16-18h at 37 °C, then
410 fixed with 10% paraformaldehyde, permeabilized with 1% tween 20, stained with rabbit
411 hyperimmune serum to rotavirus (anti-DLPs) produced in our lab and previously described ([56](#))
412 and anti-rabbit horseradish peroxidase antibody. Viral foci were stained with 3-3'-
413 diaminobenzidine and DAB Chromogen kit (Dako) and enumerated visually.

414 **Immunoblot analysis.** Cells were lysed in RIPA buffer [150 mM NaCl, 1.0% IGEPAL® CA-630,
415 0.5% sodium deoxycholate, 0.1% SDS, 50 mM Tris, pH 8.0] (Sigma-Aldrich) supplemented with

416 protease and inhibitor cocktails [1X] (Thermo Scientific™ Halt™ Protease and Phosphatase
417 Inhibitor Cocktail.100X). Proteins in cell lysates were resolved in SDS-PAGE (Mini-
418 PROTEAN® TGX™ Precast Gels [4-15%], Bio-Rad) and transferred to membranes
419 (Nitrocellulose Membrane, 0.45 µm, Bio-Rad). The membranes were blocked by incubation with
420 5% BSA, 0.1% tween 20 in phosphate-buffered saline (PBS) for 1h at room temperature and
421 with primary antibodies diluted in PBS containing 5% nonfat dry milk or 5% BSA, followed by
422 incubation with secondary, species-specific, horseradish peroxidase-conjugated antibodies. The
423 peroxidase activity was developed using the Clarity ECL substrate, Amersham Hyperfilm, and a
424 STRUCTURIX X-ray film or Azure Imager, following the manufacturer's instructions. The blots
425 were also probed with an anti-GAPDH antibody, which was used as a loading control.

426 The primaries antibodies and dilutions used were: IRF3 (CST, No. 4302, 1:1000), STAT1 (CST,
427 No. 14994, 1:1000), Phospho-Stat1, Tyr701 (CST, No. 7649, 1:1000), IFITM3 (Proteintech, No.
428 11714-1-AP, 1:1000), Mx1 (SCT, No. 37849, 1:1000), GAPDH (Proteintech, No. 60004-1,
429 1:5000). As secondary antibodies: anti-rabbit (CST, No. 7074, 1:5000) or anti-mouse (CST, No.
430 7076, 1:5000) immunoglobulin G horseradish peroxidase-linked antibodies were used.

431

432 **RNA gels.** Viral dsRNA was extracted with TRIzol (Invitrogen) according the manufacturer's
433 protocol and then mixed with Gel Loading Dye, Purple (6X), no SDS (New England Biolabs).
434 Samples were subjected to PAGE (10%) for 2.5 h at 180 Volts and visualized by ethidium
435 bromide staining (1 µg/mL) or 18h at 25 mA and silver stained using a previously described
436 method ([57](#)).

437 **Immunofluorescence analysis.** MA104 cells were infected for 24h with rRRV-GFP at a MOI of
438 0.01 FFU, then fixed with 10% paraformaldehyde, permeabilized with 1% tween 20. The cells
439 were incubated for 1 h at 37 °C temperature with an in-house rabbit anti-DLP antibody diluted at

440 1:1000. After, the cells were washed 3x with PBS and then incubated for 1h at 37 °C with
441 chicken anti-Rabbit IgG, Alexa Fluor 594 (diluted 1:2000 in 0.2% FBS-PBS). Nuclei were
442 stained with 4',6-diamidino-2-phenylindole (DAPI). Images were acquired under BZ-X Keyence
443 fluorescence microscope.

444 **Mice and RV infection.** Wild type 129sv mice were originally purchased from the Jackson
445 Laboratory and maintained as individual in house breeding colonies. 4-5 -day-old pups were
446 orally inoculated with simian RRV (10⁷ PFUs) or D6/2 (10⁴ PFUs) or recombinant simian RV
447 RRV strain (10⁷ PFUs) or rD6/2 like (1) (10⁴ PFUs) rescued using the reverse genetics method
448 described above. Fecal specimens were collected on the indicated days post infection and
449 subjected to a RT-qPCR based assay measuring RV gene NSP5 levels with standard curves to
450 determine infectious virus particles per gram of stool samples as described (45). All mice were
451 housed at the Veterinary Medical Unit of the Palo Alto VA Health Care System. All animal
452 studies were approved by the Stanford Institutional Animal Care Committee.

453 **Statistical analysis:** All experiments, unless otherwise noted, have been repeated at least
454 three times. The bar graphs are displayed as means ± SEM. Statistical significance were
455 evaluated using GraphPad Prism 7.0. or the IBM SPSS Statistics Grad Pack 26.

456

457 **Acknowledgments:** We thank all members of the Greenberg lab for their input. This work is
458 supported by a postdoctoral scholarship from CONACyT to L.S.T., the National Institutes of
459 Health (NIH) grants R01 AI125249, U19 AI116484 and by VA Merit grant GRH0022 awarded to
460 H.B.G., NIH grants K99/R00 AI135031, R01 AI150796, and an Early Career Award from the
461 Thrasher Research Fund to S.D.

462

463 **REFERENCES**

- 464 1. Crawford SE, Ramani S, Tate JE, Parashar UD, Svensson L, Hagbom M, Franco MA, Greenberg HB,
465 O’Ryan M, Kang G, Desselberger U, Estes MK. 2017. Rotavirus infection. *Nat Rev Dis Primers*
466 3:17083.
- 467 2. Burnett E, Parashar UD, Tate JE. 2020. Global impact of rotavirus vaccination on diarrhea
468 hospitalizations and deaths among children <5 years old: 2006-2019. *J Infect Dis*
469 doi:10.1093/infdis/jiaa081.
- 470 3. Estes M, Greenberg H. 2013. Rotaviruses, p1347-1401. *Fields virology*. 6 th ed. Lippincott
471 Williams & Wilkins Philadelphia,PA.
- 472 4. Lopez S, Sanchez-Tacuba L, Moreno J, Arias CF. 2016. Rotavirus Strategies Against the Innate
473 Antiviral System. *Annu Rev Virol* 3:591-609.
- 474 5. Baker JM, Tate JE, Leon J, Haber MJ, Pitzer VE, Lopman BA. 2020. Post-vaccination serum anti-
475 rotavirus immunoglobulin A as a correlate of protection against rotavirus gastroenteritis across
476 settings. *J Infect Dis* doi:10.1093/infdis/jiaa068.
- 477 6. Angel J, Steele AD, Franco MA. 2014. Correlates of protection for rotavirus vaccines: Possible
478 alternative trial endpoints, opportunities, and challenges. *Hum Vaccin Immunother* 10:3659-71.
- 479 7. Kanai Y, Komoto S, Kawagishi T, Nouda R, Nagasawa N, Onishi M, Matsuura Y, Taniguchi K,
480 Kobayashi T. 2017. Entirely plasmid-based reverse genetics system for rotaviruses. *Proc Natl*
481 *Acad Sci U S A* 114:2349-2354.
- 482 8. Malherbe H, Roux P, Kahn E. 1963. THE ROLE OF ENTEROPATHOGENIC BACTERIA AND VIRUSES
483 IN ACUTE DIARRHOEAL DISORDERS OF INFANCY AND CHILDHOOD IN JOHANNESBURG. II. 'NON-
484 SPECIFIC' GASTRO-ENTERITIS. *S Afr Med J* 37:259-61.
- 485 9. Estes MK, Graham DY, Gerba CP, Smith EM. 1979. Simian rotavirus SA11 replication in cell
486 cultures. *Journal of Virology* 31:810-815.
- 487 10. Yin N, Yang FM, Qiao HT, Zhou Y, Duan SQ, Lin XC, Wu JY, Xie YP, He ZL, Sun MS, Li HJ. 2018.
488 Neonatal rhesus monkeys as an animal model for rotavirus infection. *World J Gastroenterol*
489 24:5109-5119.
- 490 11. Ramig RF. 1988. The effects of host age, virus dose, and virus strain on heterologous rotavirus
491 infection of suckling mice. *Microb Pathog* 4:189-202.
- 492 12. Komoto S, Fukuda S, Kugita M, Hatazawa R, Koyama C, Katayama K, Murata T, Taniguchi K. 2019.
493 Generation of Infectious Recombinant Human Rotaviruses from Just 11 Cloned cDNAs Encoding
494 the Rotavirus Genome. *J Virol*;93(8):e02207-18.
- 495 13. Kawagishi T, Nurdin JA, Onishi M, Nouda R, Kanai Y, Tajima T, Ushijima H, Kobayashi T. 2020.
496 Reverse Genetics System for a Human Group A Rotavirus. *J Virol*;94(2):e00963-19.
- 497 14. Falkenhagen A, Patzina-Mehling C, Gadicherla AK, Strydom A, O’Neill HG, Johne R. 2020.
498 Generation of Simian Rotavirus Reassortants with VP4- and VP7-Encoding Genome Segments
499 from Human Strains Circulating in Africa Using Reverse Genetics. *Viruses*;12(2):201.
- 500 15. Falkenhagen A, Patzina-Mehling C, Ruckner A, Vahlenkamp TW, Johne R. 2019. Generation of
501 simian rotavirus reassortants with diverse VP4 genes using reverse genetics. *J Gen Virol*
502 100:1595-1604.
- 503 16. Philip AA, Perry JL, Eaton HE, Shmulevitz M, Hyser JM, Patton JT. 2019. Generation of
504 Recombinant Rotavirus Expressing NSP3-UnaG Fusion Protein by a Simplified Reverse Genetics
505 System. *J Virol*;93(24):e01616-19
- 506 17. Komoto S, Fukuda S, Ide T, Ito N, Sugiyama M, Yoshikawa T, Murata T, Taniguchi K. 2018.
507 Generation of Recombinant Rotaviruses Expressing Fluorescent Proteins by Using an Optimized
508 Reverse Genetics System. *J Virol*;92(13):e00588-18.
- 509 18. Philip AA, Herrin BE, Garcia ML, Abad AT, Katen SP, Patton JT. 2019. Collection of Recombinant
510 Rotaviruses Expressing Fluorescent Reporter Proteins. *Microbiol Resour Announc*;8(27):e00523-
511 19.

- 512 19. Ramig RF. 2004. Pathogenesis of intestinal and systemic rotavirus infection. *J Virol* 78:10213-20.
513 20. Feng N, Kim B, Fenaux M, Nguyen H, Vo P, Omary MB, Greenberg HB. 2008. Role of interferon in
514 homologous and heterologous rotavirus infection in the intestines and extraintestinal organs of
515 suckling mice. *J Virol* 82:7578-90.
516 21. Ramani S, Crawford SE, Blutt SE, Estes MK. 2018. Human organoid cultures: transformative new
517 tools for human virus studies. *Current opinion in virology* 29:79-86.
518 22. Saxena K, Blutt SE, Ettayebi K, Zeng XL, Broughman JR, Crawford SE, Karandikar UC, Sastri NP,
519 Conner ME, Opekun AR, Graham DY, Qureshi W, Sherman V, Foulke-Abel J, In J, Kovbasnjuk O,
520 Zachos NC, Donowitz M, Estes MK. 2016. Human Intestinal Enteroids: a New Model To Study
521 Human Rotavirus Infection, Host Restriction, and Pathophysiology. *J Virol* 90:43-56.
522 23. Saxena K, Simon LM, Zeng X-L, Blutt SE, Crawford SE, Sastri NP, Karandikar UC, Ajami NJ, Zachos
523 NC, Kovbasnjuk O, Donowitz M, Conner ME, Shaw CA, Estes MK. 2017. A paradox of
524 transcriptional and functional innate interferon responses of human intestinal enteroids to
525 enteric virus infection. *Proceedings of the National Academy of Sciences* 114:E570.
526 24. Feng N, Yasukawa LL, Sen A, Greenberg HB. 2013. Permissive replication of homologous murine
527 rotavirus in the mouse intestine is primarily regulated by VP4 and NSP1. *J Virol* 87:8307-16.
528 25. Feng N, Sen A, Wolf M, Vo P, Hoshino Y, Greenberg HB. 2011. Roles of VP4 and NSP1 in
529 determining the distinctive replication capacities of simian rotavirus RRV and bovine rotavirus
530 UK in the mouse biliary tract. *J Virol* 85:2686-94.
531 26. Ding S, Zhu S, Ren L, Feng N, Song Y, Ge X, Li B, Flavell RA, Greenberg HB. 2018. Rotavirus VP3
532 targets MAVS for degradation to inhibit type III interferon expression in intestinal epithelial cells.
533 *Elife*;7:e39494.
534 27. Burns JW, Krishnaney AA, Vo PT, Rouse RV, Anderson LJ, Greenberg HB. 1995. Analyses of
535 homologous rotavirus infection in the mouse model. *Virology* 207:143-53.
536 28. Greenberg HB, Vo PT, Jones R. 1986. Cultivation and characterization of three strains of murine
537 rotavirus. *J Virol* 57:585-90.
538 29. Jais PH, Decroly E, Jacquet E, Le Boulch M, Jais A, Jean-Jean O, Eaton H, Ponien P, Verdier F,
539 Canard B, Goncalves S, Chiron S, Le Gall M, Mayeux P, Shmulevitz M. 2019. C3P3-G1: first
540 generation of a eukaryotic artificial cytoplasmic expression system. *Nucleic Acids Res* 47:2681-
541 2698.
542 30. Schoggins JW, Rice CM. 2011. Interferon-stimulated genes and their antiviral effector functions.
543 *Curr Opin Virol* 1:519-25.
544 31. Arnold MM, Sen A, Greenberg HB, Patton JT. 2013. The battle between rotavirus and its host for
545 control of the interferon signaling pathway. *PLoS Pathog* 9:e1003064.
546 32. Sen A, Rothenberg ME, Mukherjee G, Feng N, Kalisky T, Nair N, Johnstone IM, Clarke MF,
547 Greenberg HB. 2012. Innate immune response to homologous rotavirus infection in the small
548 intestinal villous epithelium at single-cell resolution. *Proc Natl Acad Sci U S A* 109:20667-72.
549 33. Whitaker AM, Hayward CJ. 1985. The characterization of three monkey kidney cell lines. *Dev*
550 *Biol Stand* 60:125-31.
551 34. Precious BL, Carlos TS, Goodbourn S, Randall RE. 2007. Catalytic turnover of STAT1 allows PIV5
552 to dismantle the interferon-induced anti-viral state of cells. *Virology* 368:114-21.
553 35. Didcock L, Young DF, Goodbourn S, Randall RE. 1999. The V protein of simian virus 5 inhibits
554 interferon signalling by targeting STAT1 for proteasome-mediated degradation. *J Virol* 73:9928-
555 33.
556 36. Peterhans E, Schweizer M. 2013. BVDV: a pestivirus inducing tolerance of the innate immune
557 response. *Biologicals* 41:39-51.
558 37. Seago J, Hilton L, Reid E, Doceul V, Jeyatheesan J, Moganeradj K, McCauley J, Charleston B,
559 Goodbourn S. 2007. The Npro product of classical swine fever virus and bovine viral diarrhea

- 560 virus uses a conserved mechanism to target interferon regulatory factor-3. *J Gen Virol* 88:3002-
561 6.
- 562 38. Childs KS, Andrejeva J, Randall RE, Goodbourn S. 2009. Mechanism of mda-5 Inhibition by
563 paramyxovirus V proteins. *J Virol* 83:1465-73.
- 564 39. Childs K, Randall R, Goodbourn S. 2012. Paramyxovirus V proteins interact with the RNA Helicase
565 LGP2 to inhibit RIG-I-dependent interferon induction. *J Virol* 86:3411-21.
- 566 40. Sen A, Pruijssers AJ, Dermody TS, Garcia-Sastre A, Greenberg HB. 2011. The early interferon
567 response to rotavirus is regulated by PKR and depends on MAVS/IPS-1, RIG-I, MDA-5, and IRF3. *J*
568 *Virol* 85:3717-32.
- 569 41. Meade NJ. 2016. INTERVENTION STRATEGIES AGAINST ROTAVIRUS IN PIGS. Doctor of
570 Philosophy. University of Nottingham, Nottingham, UK.
- 571 42. Esona MD, Foytich K, Wang Y, Shin G, Wei G, Gentsch JR, Glass RI, Jiang B. 2010. Molecular
572 characterization of human rotavirus vaccine strain CDC-9 during sequential passages in Vero
573 cells. *Hum Vaccin*;6(3):10409.
- 574 43. Eaton HE, Kobayashi T, Dermody TS, Johnston RN, Jais PH, Shmulevitz M. 2017. African Swine
575 Fever Virus NP868R Capping Enzyme Promotes Reovirus Rescue during Reverse Genetics by
576 Promoting Reovirus Protein Expression, Virion Assembly, and RNA Incorporation into Infectious
577 Virions. *J Virol*;91(11):e02416-16.
- 578 44. Feng N, Franco MA, Greenberg HB. 1997. Murine model of rotavirus infection. *Adv Exp Med Biol*
579 412:233-40.
- 580 45. Feng N, Kim B, Fenaux M, Nguyen H, Vo P, Omary MB, Greenberg HB. 2008. Role of Interferon in
581 Homologous and Heterologous Rotavirus Infection in the Intestines and Extraintestinal Organs
582 of Suckling Mice. *Journal of Virology* 82:7578-7590.
- 583 46. Ramig RF. 2007. Systemic rotavirus infection. *Expert Review of Anti-infective Therapy* 5:591-612.
- 584 47. Hertel PM, Estes MK. 2012. Rotavirus and biliary atresia: can causation be proven? *Curr Opin*
585 *Gastroenterol* 28:10-7.
- 586 48. Mohanty SK, Donnelly B, Temple H, Tiao GM. 2019. A Rotavirus-Induced Mouse Model to Study
587 Biliary Atresia and Neonatal Cholestasis, p 259-271. *In* Vinken M (ed), *Experimental Cholestasis*
588 *Research* doi:10.1007/978-1-4939-9420-5_17. Springer New York, New York, NY.
- 589 49. Ortiz-Perez A, Donnelly B, Temple H, Tiao G, Bansal R, Mohanty SK. 2020. Innate Immunity and
590 Pathogenesis of Biliary Atresia. *Front Immunol.* 2020;11:329.
- 591 50. Jiang B, Gentsch JR, Glass RI. 2002. The Role of Serum Antibodies in the Protection against
592 Rotavirus Disease: An Overview. *Clinical Infectious Diseases* 34:1351-1361.
- 593 51. Resch TK, Wang Y, Moon S, Jiang B. 2020. Serial passaging of human rotavirus CDC-9 strain in
594 cell culture leads to attenuation: characterization from in vitro and in vivo studies. *J Virol*
595 doi:10.1128/jvi.00889-20.
- 596 52. Buchholz UJ, Finke S, Conzelmann KK. 1999. Generation of bovine respiratory syncytial virus
597 (BRSV) from cDNA: BRSV NS2 is not essential for virus replication in tissue culture, and the
598 human RSV leader region acts as a functional BRSV genome promoter. *J Virol* 73:251-9.
- 599 53. Nair N, Feng N, Blum LK, Sanyal M, Ding S, Jiang B, Sen A, Morton JM, He XS, Robinson WH,
600 Greenberg HB. 2017. VP4- and VP7-specific antibodies mediate heterotypic immunity to
601 rotavirus in humans. *Sci Transl Med.* 2017;9(395):eaam5434.
- 602 54. Hoshino Y, Wyatt RG, Greenberg HB, Flores J, Kapikian AZ. 1984. Serotypic similarity and
603 diversity of rotaviruses of mammalian and avian origin as studied by plaque-reduction
604 neutralization. *J Infect Dis* 149:694-702.
- 605 55. Jiang *et al.* September 2014. HUMAN ROTAVIRUS VACCINE STRAINS AND DIAGNOSTICS. US
606 patent 9,498,526 B2.

- 607 56. Feng N, Lawton JA, Gilbert J, Kuklin N, Vo P, Prasad BVV, Greenberg HB. 2002. Inhibition of
608 rotavirus replication by a non-neutralizing, rotavirus VP6-specific IgA mAb. *The Journal of*
609 *Clinical Investigation* 109:1203-1213.
- 610 57. Herring AJ, Inglis NF, Ojeh CK, Snodgrass DR, Menzies JD. 1982. Rapid diagnosis of rotavirus
611 infection by direct detection of viral nucleic acid in silver-stained polyacrylamide gels. *Journal of*
612 *clinical microbiology* 16:473-477.

613
614
615
616
617
618
619
620
621
622

623 **FIGURE LEGENDS**

624

625 **Figure 1:** *MA104 N*V cell line characterization.* **(A)** Representative Immunoblot of cellular
626 targets of N and V viral proteins in wild type (wt) and modified MA104 cells. Stable cell lines
627 expressing N, V, or N and V proteins and wtMA104 cell lines were analyzed by immunoblot and
628 the expression of STAT1 and IRF3 were detected with the indicated antibodies. GAPDH
629 detection was used as a loading control. **(B)** wt and MA104 N*V cells were pretreated with or
630 without 800 UI/mL of IFN- α for 30 min or 16 h and then processed for immunoblot. The
631 expression of pSTAT1 (Tyr 701), IRF3, STAT1, IFITM3 and Mx1 was detected with the
632 indicated antibodies. GAPDH detection was used as a loading control.

633
634

635 **Figure 2:** *MA104 N*V cells support higher levels of RV replication.* **(A)** MA104 and MA104 N*V
636 cells were infected with the indicated RV strains at MOI of 1. At 24 hpi, cells were lysed, and
637 virus titers determined by an immunoperoxidase focus-forming assay. **(B)** MA104 wt and N*V
638 cells, pretreated with or without 800 UI/mL of IFN- α for 16 h were infected with indicated RV
639 strains (MOI=0.01). At the indicated time points, total RNA was harvested and RV NSP5 mRNA
640 levels were measured by RT-qPCR and normalized to GAPDH. The arithmetic means \pm
641 standard deviations from three **(A)** or two **(B)** independent experiments are shown. Statistical
642 significance was evaluated by student's t-test. The asterisks indicate significant differences (* $p \leq$
643 0.05; ** $p \leq$ 0.01; *** $p \leq$ 0.001).

644
645

646 **Figure 3:** Schematic representation of an improved reverse genetics system for RVs recovery
647 including the use of N*V modified MA104 cells and the C3P3-G1 plasmid.

648
649

650 **Figure 4: Rotavirus dsRNA genomic profiles by RNA-PAGE.** Viral RNA extracted from MA104
651 cells infected with indicated RVs and then separated on a 10% polyacrylamide gel and stained
652 by ethidium bromide. The position of segments of interest are marked with red asterisks. The
653 dsRNA segment numbers are shown in the figure.

654
655

656 **Figure 5: Recovery of the recombinant RRV (rRRV) and the fluorescent RRV (rRRV-GFP).** (A)
657 pT7 organization of wild type NSP3 and GFP-NSP3 RRV, nucleotide positions are labeled. (B)
658 Genetic stability of rRRV (blue) and rRRV-GFP (green). The recombinants rotaviruses were
659 serially passaged 5 times in MA104 cells. Cells were harvest at day 5 post infection or when
660 complete cytopathic effects were observed, the virus titer was determined by an
661 immunoperoxidase focus forming assay. (C) Additionally, rRRV-GFP was passaged 8 times in
662 MA104 cells, RNA viral from all passages (2-8) was extracted and separated on a 10%
663 polyacrylamide gel and stained by ethidium bromide. The position of engineered segment 7 is
664 marked with red arrowheads. The segment numbers are shown in the figure. (D) Replication
665 kinetics of wtRRV, rRRV and rRRV-GFP. Monolayers of MA104 cells were infected with RVs at
666 an MOI of 0.01 a in the presence of trypsin (0.5 µg/mL) and then were harvest at indicated times
667 by freezing/thawing. The viral titers were determined by immunoperoxidase focus forming
668 assay. Results are expressed as the mean viral titer from triplicate experiments. Error bars
669 shown the SD. (E) Comparison of plaques size. Plaques were generated on MA104 monolayers
670 and detected at 3 dpi by crystal violet staining. Representative photographs of viral plaques are
671 shown. The sizes of at least 24 randomly selected plaques from 2 independent plaque assays
672 were measured using the GraphPad Prism v7 and reported as area on relative units. Mean
673 values and the standard deviation are shown. Statistical significance was evaluated by student's
674 t-test. The asterisks indicate significant differences (*ns*: not significant, * $p \leq 0.05$; ** $p \leq 0.01$; *** p
675 ≤ 0.001). (F) Subcellular localization of GFP protein in rRRV-GFP infected cells. MA104 cells
676 were infected with rRRV-GFP at MOI of 0.01. After 24 hpi, infected cells were fixed and
677 visualized by fluorescence microscopy. Using anti-VP6 polyclonal antiserum and the Alexa
678 Fluor 594 anti-rabbit IgG, nuclei were stained with DAPI. Scale bar: 50 µm.

679
680

681 **Figure 6: Characterization of rRVs in an in vivo mice model.** Five-day-old 129sv mouse were
682 orally inoculated with 10^7 PFUs of simian wtRRV or rRRV (A-B) or 10^4 PFUs of D6/2 or rD6/2
683 like (1) RV (C-D). Diarrhea was monitored from days 1 to 8 post infection and fecal specimens
684 were collected on the indicated dpi and examined by RT-qPCR-based assay measuring RV
685 gene NSP5 levels with standard curves as a measure of RV shedding per mg of stool. The
686 numbers of mice in each group are indicated in parentheses. (E) dsRNA genomic profile from
687 rD6/2 RV was confirmed by RNA-PAGE. The position of segments of interest are marked with
688 red arrowheads. The segment numbers are shown in the figure. Statistical significance was
689 evaluated by student's t-test. The asterisks indicate significant differences (*ns*: not significant * p
690 ≤ 0.05 ; ** $p \leq 0.01$; *** $p \leq 0.001$).

691
692
693

694 **TABLE LEGENDS**

695

696

697 **Table 1:** Comparison of RG rescue frequencies for different RV strains and for modified RV
698 using Kanai^{*}, Komoto^{*} and the improved RV system including MA104 N*V cells and the C3P3-
699 G1 plasmid. Statistical significance was evaluated by Chi square method. The asterisks indicate
700 significant differences (*p ≤ 0.05; **p ≤ 0.01; ***p ≤ 0.001).

701 ⁰ Numbers in parenthesis: the first number represents the number of successful rescues and the
702 second one the total number of attempts.

703 ^{*}Modified version.

704

705

706

707

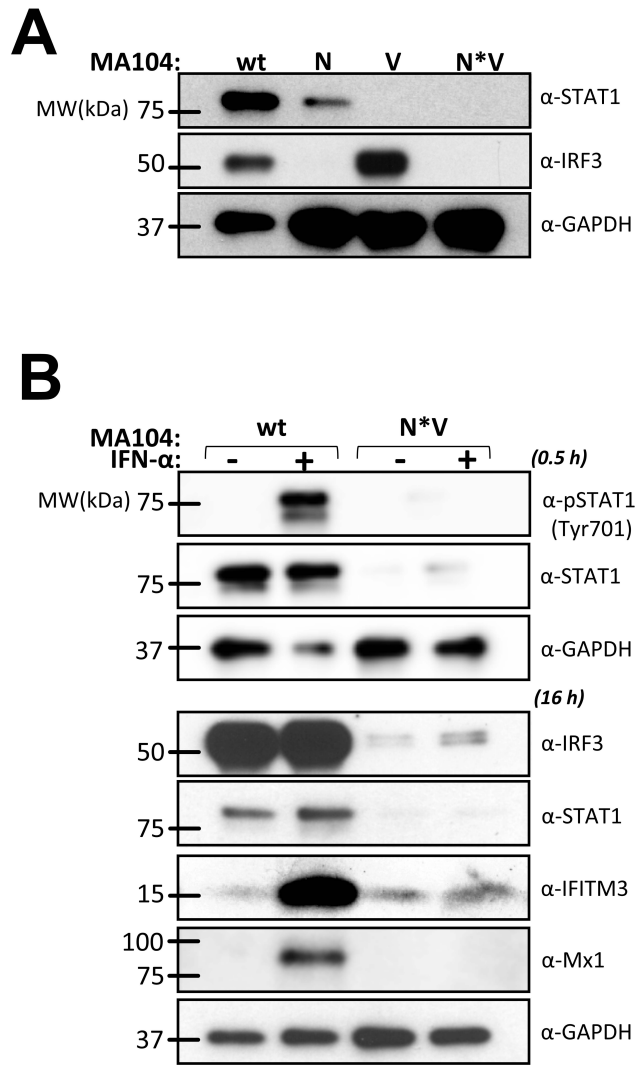
708

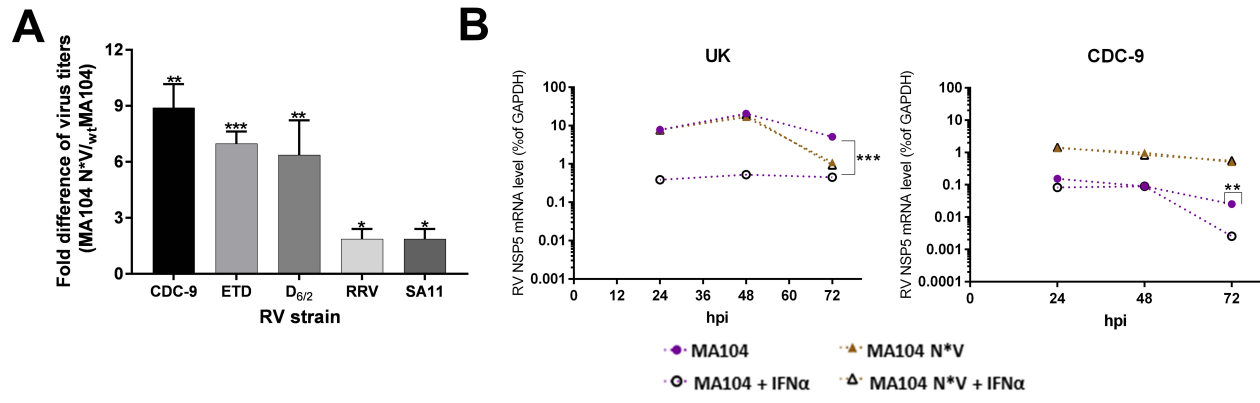
Table 1: Comparison of RG rescue frequencies for different RV strains and for modified RVs using Kanai*, Komoto* and the improved RV system including MA104 N*V cells and the C3P3-G1 plasmid. Statistical significance was evaluated by Chi square method. The asterisks indicate significant differences (* $p \leq 0.05$; ** $p \leq 0.01$; *** $p \leq 0.001$).

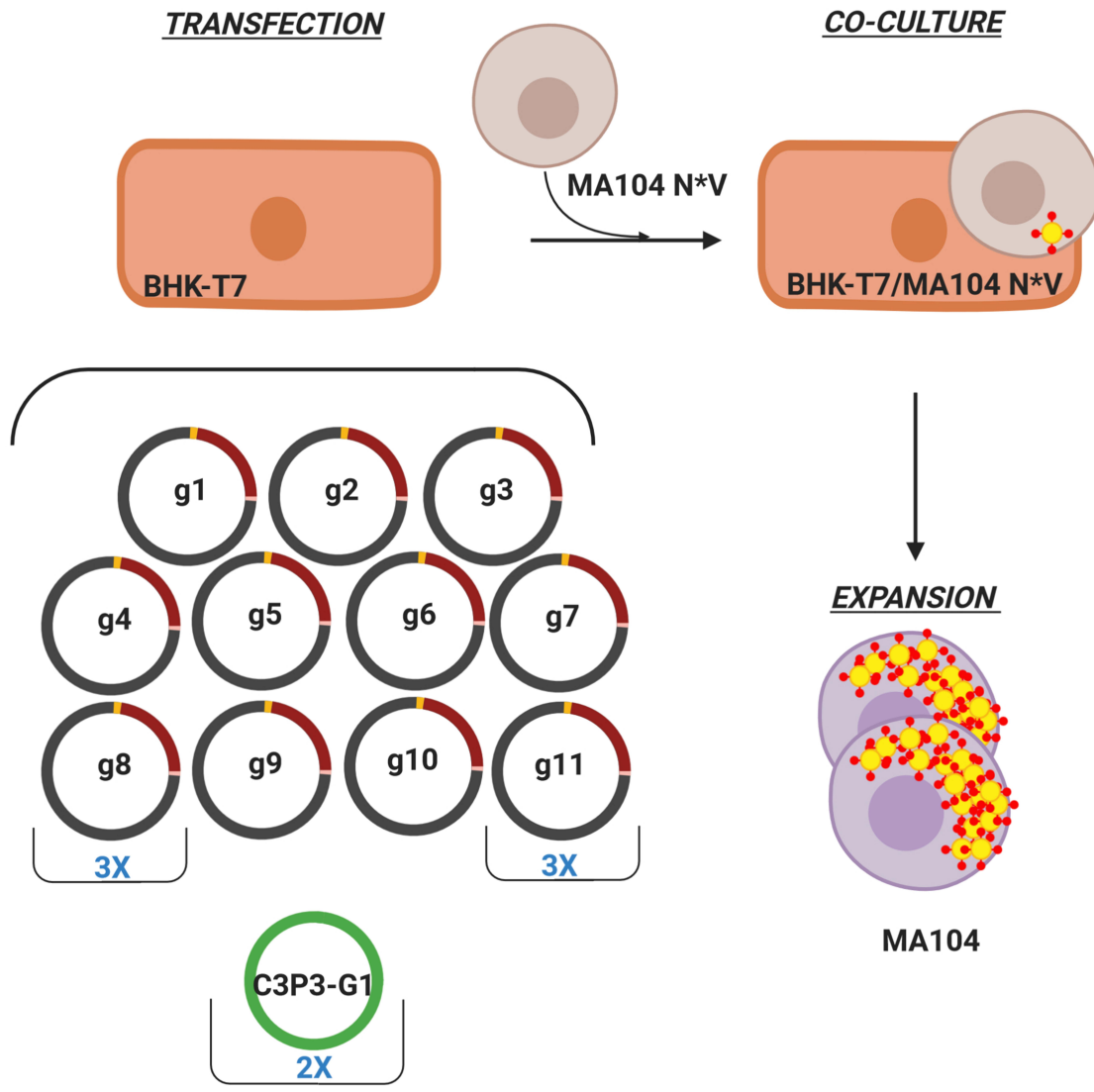
Recombinant RV Strain		Rescue efficiency (%)		
		*Kanai	*Komoto	Improved
<i>Human</i>	rCDC-9	0 (0/2)	0 (0/8)	100*** (5/5)
	rCDC-9/UK_VP4	0 (0/2)	0 (0/6)	100*** (5/5)
<i>Simian</i>	rSA11	100 (3/3)	100 (3/3)	100 (3/3)
	rRRV	0 (0/3)	16.7 (1/6)	83.3** (5/6)
	rRRV-GFP	0 (0/3)	16.7 (1/6)	100*** (6/6)
<i>Murine-like</i>	SA11 X D6/2 reassortment [rD6/2 like (1)]	0 (0/2)	8.3 (1/12)	80** (4/5)

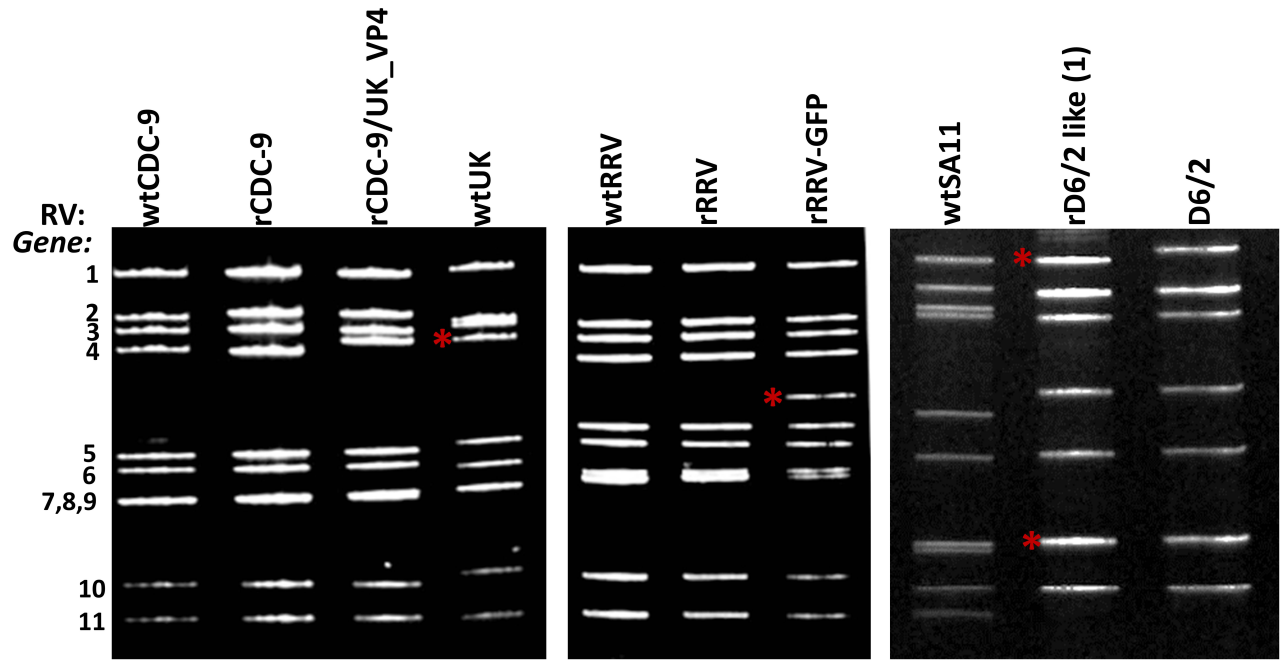
⁰ Numbers in parenthesis: the first number represents the number of successful rescues and the second one the total number of attempts.

*Modified version.

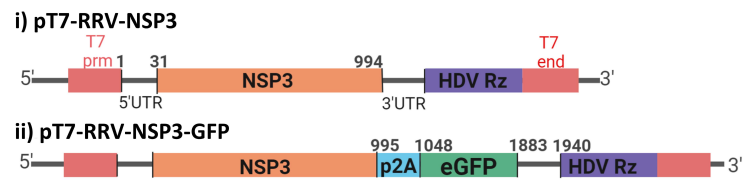




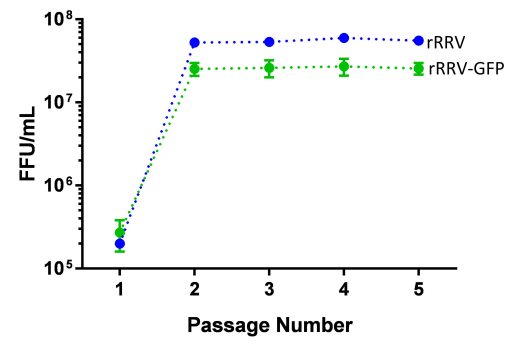




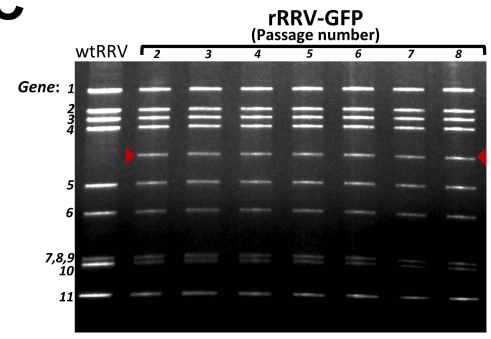
A



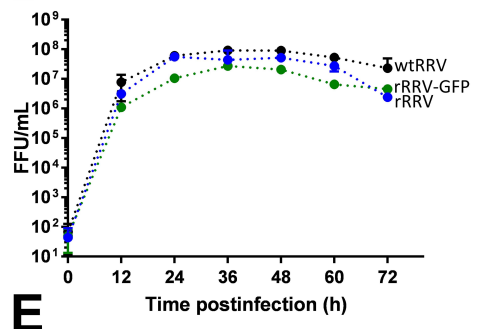
B



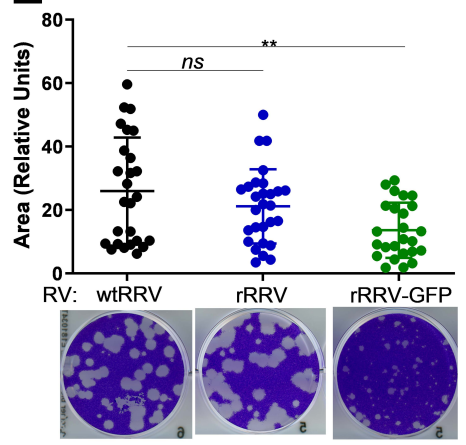
C



D



E



F

